A New Optimal Power Flow Model Considering the Active Power Constraints of Transmission Interfaces

XIUQIONG HU
School of Information and Electric Engineering,
Panzhihua University,
Panzhihua, 617000,
CHINA

Abstract: - An optimal power flow model as well as algorithm is provided for interconnected power systems considering active power constraints of transmission interfaces. To ensure the optimum operation of an interconnected power system, the optimal goal of the proposed model is minimizing the loss of active power. For satisfying transaction power constraints, the active power constraints of transmission interfaces are taken into account as inequality constraints. Considering the multi-area characteristic of interconnected power systems, a decomposition-coordination optimal model is proposed on the base of the model previously established. And the decomposition-coordination interior point method is used to solve the decomposition-coordination optimal model. Simulations of two test systems illustrate that the proposed model as well as the algorithm can improve computational efficiency, which can provide operation schedule decisions for interconnected power systems.

Key-Words: - Interconnected Power System, Optimal Power Flow, Active Power Constraints of Transmission Interfaces, Decomposition-coordination Optimal Model, Decomposition-coordination Interior Point Method, computational efficiency

Received: April 6, 2022. Revised: February 8, 2023. Accepted: March 10, 2023. Published: April 11, 2023.

1 Introduction

Under the power market environment, the interconnection of power grids becomes the developing direction for the power system. In the interconnected power system, though each area has its independent system operation, it still needs to be controlled coordinately to guarantee optimal operation of the system. These situations provide an opportunity for the development of optimal power flow. At present, optimal power flow is mainly used for pricing, [1], [2], [3], congestion management, [4], [5], [6], [7], available transfer capability, [8], [9], etc. For interconnected power systems, however, to achieve a wider range of optimal assignment of resources, and greater competition in the market, the active power of transmission interfaces must also be adjusted to the specified value to meet the transaction power constraints. However, this is barely considered in the present optimal power flow model.

The calculation methods of optimal power flow include the centralized algorithm, [10], [11], [12], and the distributed algorithm, [1], [4], [5], [13], [14], [15]. In the interconnected power system, the centralized algorithm has difficulty in real-time data collection, and disadvantages of heterogeneous data resources, large data traffic, and large data storage. Whereas the distributed algorithm can complete calculations independently, according to the local data and target within each area. So, the distributed algorithm has the advantages of small data traffic and small data storage, and it can guarantee the global simulation precision and speed requirements while avoiding the leak of internal important data. Therefore, the distributed algorithm becomes an important calculation tool to solve the integration simulation for the interconnected power system.

For the distributed algorithms, the auxiliary problem principle (APP) algorithm is widely used, [13], [14]. However, the research of APP is not yet mature. In [15], decomposition-coordination interior point method was compared with the APP algorithm, and found that this method was better than the APP algorithm in computing time, the accuracy of the objective function, and iteration number.

Based on existing research, an optimal power flow model, as well as the algorithm is proposed considering the active power constraints of transmission interfaces. This model uses minimizing the loss of active power as an optimization goal. And the inequality constraints include active power constraints of transmission interfaces. Then, considering the disadvantages of the centralized algorithm and APP, the decomposition-coordination model is established, and calculated by the decomposition-coordination interior point method.

2 The Proposed Optimal Power Flow Model

To take into account the optimal economic operation for the power system, the proposed optimal power flow model uses minimizing the loss of active power as an optimization goal. The optimized variables include the reactive power generated by the generator, the active power generated by the generator, the reactive power output of shunt reactive power compensation equipment, the ratio of transformer fitted with an on-load tap changer (OLTC) as well as bus voltage. All constraints include the power flow equality constraints, the active power constraints of transmission interfaces, and the inequality constraints of optimized variables.

The proposed optimal power flow model can be formulated by Equations (1)-(12).

$$\min \quad \sum_{i\in N_{\mathrm{B}}} P_{\mathrm{G}i} - \sum_{i\in N_{\mathrm{B}}} P_{\mathrm{D}i} \tag{1}$$

s.t

$$P_{\mathrm{G}i} - P_{\mathrm{D}i} - \sum_{ij\in S_{\mathrm{L}i}} P_{\mathrm{L}ij} - \sum_{ij\in S_{\mathrm{T}i}} P_{\mathrm{T}ij} = 0 \qquad i\in N_{\mathrm{B}} \tag{2}$$

$$Q_{\mathrm{G}i} + Q_{\mathrm{C}i} + Q_{\mathrm{R}i} - Q_{\mathrm{D}i} - \sum_{ij\in S_{\mathrm{L}i}} Q_{\mathrm{L}ij} - \sum_{ij\in S_{\mathrm{T}i}} Q_{\mathrm{T}ij} = 0 \qquad i\in N_{\mathrm{B}} \tag{3}$$

$$e_i f_m - e_m f_i = 0 \qquad i,m\in N_{\mathrm{T}} \tag{4}$$

$$e_i - k_t e_m = 0 \qquad i,m,t\in N_{\mathrm{T}} \tag{5}$$

$$\sum_{ij\in S_{\mathrm{link},n}} P_{ij,n} - P_{\mathrm{cut},n} = 0 \qquad n\in N_{\mathrm{cut}} \tag{6}$$

$$V_{i\min}^2 \le V_i^2 = e_i^2 + f_i^2 \le V_{i\max}^2 \qquad i\in N_{\mathrm{B}} \tag{7}$$

$$k_{t\min} \le k_t \le k_{t\max} \qquad t\in N_{\mathrm{T}} \tag{8}$$

$$Q_{\mathrm{G}i\min} \le Q_{\mathrm{G}i} \le Q_{\mathrm{G}i\max} \qquad i\in N_{\mathrm{G}} \tag{9}$$

$$Q_{\mathrm{C}i\min} \le Q_{\mathrm{C}i} \le Q_{\mathrm{C}i\max} \qquad i\in N_{\mathrm{C}} \tag{10}$$

$$Q_{\mathrm{R}i\min} \le Q_{\mathrm{R}i} \le Q_{\mathrm{R}i\max} \qquad i\in N_{\mathrm{R}} \tag{11}$$

$$P_{\mathrm{G}i\min} \le P_{\mathrm{G}i} \le P_{\mathrm{G}i\max} \qquad i\in N_{\mathrm{G}} \tag{12}$$

In the above equations, N_{B}, N_{G}, N_{T}, N_{C}, N_{R}, and N_{cut} respectively represent the number of buses, generators, and transformers fitted with OLTC, shunt capacitor, shunt reactor, and transmission interface. $S_{\mathrm{link},n}$, $S_{\mathrm{L}i}$, *and* $S_{\mathrm{T}i}$ respectively represent the set of tie lines included in the nth transmission interface, line branch connected with ith bus, and OLTC connected with ith bus. P_{G}, Q_{G}, P_{D}, Q_{D}, Q_{C}, Q_{R}, k, V, e, and f respectively represent the active power generated by the generator, the reactive power generated by the generator, the active load, the reactive load, the reactive power generated by shunt capacitor, the reactive power generated by shunt reactor, the ratio of transformer fitted with OLTC, the amplitude of bus voltage, the real parts and imaginary parts of bus voltage. $P_{\mathrm{L}ij}$, $Q_{\mathrm{L}ij}$, $P_{\mathrm{T}ij}$, and $Q_{\mathrm{T}ij}$ respectively represent the active power and reactive power of the line branch, and the active power and reactive power of the branch with a transformer fitted with OLTC. $P_{ij,n}$ represents the active power of the nth transmission interface. $P_{\mathrm{cut},n}$ represents the set value of transaction power for the nth transmission interface.

Furthermore, Equations (2) and (3) represent power flow equality constraints; Equations (4) and (5) represent the voltage conversion relation of branches with transformer fitted with OLTC; Equation (6) represents the active power constraints of transmission interfaces; Equations (7)-(12) respectively represent the inequality constraints for each optimized variable.

The present interconnected power system has characteristics of hierarchical and partition management, and each dispatching center is only responsible for the maintenance and management of its data. If the above model uses the traditional centralized optimization algorithm, it is bound to encounter the splicing problem of basic data. Especially, when the scale of interconnected power is increasing, the above model could meet the convergence problem. The decomposition-coordination algorithm based on multi-area can well solve these problems.

3 The Decomposition-coordination Model and Algorithm

3.1 The Decomposition-coordination Model

Using a two-area interconnected power system, for example, $\boldsymbol{x}_{\mathrm{I1}}$, and $\boldsymbol{x}_{\mathrm{I2}}$ respectively represent the inner variables of each area without boundary buses, and $\boldsymbol{x}_{\mathrm{B}}$ represents the variable of boundary buses. And for area 1, the variable of boundary buses can be denoted as $\boldsymbol{x}_{\mathrm{B1}} = (e_{i_1}, f_{i_1}, P_{i_1}, Q_{i_1})^{\mathrm{T}}$; for area 2, the variable of boundary buses can be denoted as $\boldsymbol{x}_{\mathrm{B2}} = (e_{i_2}, f_{i_2}, P_{i_2}, Q_{i_2})^{\mathrm{T}}$. The specific decomposition-coordination model can be expressed by Equations (13) - (18).

$$\min \quad f_1(\boldsymbol{x}_{\mathrm{I1}}, \boldsymbol{x}_{\mathrm{B1}}) + f_2(\boldsymbol{x}_{\mathrm{I2}}, \boldsymbol{x}_{\mathrm{B2}}) \tag{13}$$

$$s.t. \quad \boldsymbol{g}_1(\boldsymbol{x}_{\mathrm{I1}}, \boldsymbol{x}_{\mathrm{B1}}) = 0 \tag{14}$$

$$\boldsymbol{g}_2(\boldsymbol{x}_{\mathrm{I2}}, \boldsymbol{x}_{\mathrm{B2}}) = 0 \tag{15}$$

$$\underline{\boldsymbol{h}_1} \le \boldsymbol{h}_1(\boldsymbol{x}_{\mathrm{I1}}, \boldsymbol{x}_{\mathrm{B1}}) \le \overline{\boldsymbol{h}_1} \tag{16}$$

$$\underline{\boldsymbol{h}_2} \le \boldsymbol{h}_2(\boldsymbol{x}_{\mathrm{I2}}, \boldsymbol{x}_{\mathrm{B2}}) \le \overline{\boldsymbol{h}_2} \tag{17}$$

$$\boldsymbol{x}_{\mathrm{B1}} - \boldsymbol{x}_{\mathrm{B2}} = 0 \tag{18}$$

In the above equations, Equation (13) represents the sum of the objective function of each area which can be expressed by Equation (1); Equation (14) and Equation (15) respectively represent the equality constraints for area1 and area2; Equation (16) and Equation (17) respectively represent the inequality constraints for area1 and area2; Equation (18), which is the boundary coordination equation, represents the coupling constraints for the two areas, and it can be further stated as Equation (19).

$$\sum_m \boldsymbol{A}_m \boldsymbol{x}_m = 0 \qquad m \in N_{\mathrm{A}} \tag{19}$$

In Equation (19), N_{A} represents the number of areas, $\boldsymbol{A}_m$ represents the coupling relationship matrix between area m and the other areas, and $\boldsymbol{x}_m$ represents the variables which include the inner variables and boundary variables.

3.2 The Solving Steps based on Decomposition-coordination Interior Point Method

Decomposition-coordination interior-point method, which was proposed in [13], is used to solve Equations (13)-(19). The solving steps are shown below.

1) Iteration number donated by K for the decomposition-coordination interior point method should be set as 0 and its maximum value is given. The tolerance error for complementary gap and KT condition are set as 10^{-6}. The initial values of variables and the Lagrange multiplier are determined.

2) The complementary gap and residue of the optimal model for each area are calculated. And if they are less than the set tolerance error, the solution will stop, and the optimal value is achieved. Otherwise, it will turn to step 3).

3) The K is set as K + 1. If K is greater than the maximum number of iterations for the decomposition-coordination interior point method, it shows the solution is not converged, and the solution will stop. Otherwise, it will turn to step 4).

4) According to the following steps, the original variables and the dual variables for each area will be updated:

- According to the Jacobin matrix and Hessian matrix of each area, the correction equation $\boldsymbol{M}_m$ and residue $\boldsymbol{B}_m$ with reduced order are solved.
- Combined with the coupling relationship matrix $\boldsymbol{A}_m$, the matrix $\boldsymbol{E}_m = [\boldsymbol{A}_m, \boldsymbol{0}_{q \times N_m}]$, in which N_m and q respectively represent the number of equality constraints and coupling constraints, is achieved.
- According to the following equation $(-\boldsymbol{E}_1\boldsymbol{M}_1^{-1}\boldsymbol{E}_1^{\mathrm{T}} - \ldots - \boldsymbol{E}_{N_{\mathrm{A}}}\boldsymbol{M}_{N_{\mathrm{A}}}^{-1}\boldsymbol{E}_{N_{\mathrm{A}}}^{\mathrm{T}})\Delta\boldsymbol{y}_{\mathrm{d}} = \boldsymbol{E}_1\boldsymbol{M}_1^{-1}\boldsymbol{B}_1^{\mathrm{T}} + \ldots + \boldsymbol{E}_{N_{\mathrm{A}}}\boldsymbol{M}_{N_{\mathrm{A}}}^{-1}\boldsymbol{B}_{N_{\mathrm{A}}}^{\mathrm{T}} - \boldsymbol{D}_{\mathrm{d}}$, $\Delta\boldsymbol{y}_{\mathrm{d}}$, which is the Lagrange multiplier of coupling constraints, is calculated.
- After that, according to the following equation $\boldsymbol{M}_m \times [\Delta\boldsymbol{x}_m, \Delta\boldsymbol{y}_m]^{\mathrm{T}} = -\boldsymbol{B}_m - \boldsymbol{E}_m^{\mathrm{T}}\Delta\boldsymbol{y}_{\mathrm{d}}$, the increment of the optimal variable for each area can be achieved. In this equation, $\boldsymbol{y}_m$ represents the Lagrange multiplier of equality constraints.
- According to the iterative step and the increment of the optimal variable for each area, the optimal variables can be updated.

5) Return to step 2).

Detailed steps of the decomposition-coordination interior-point method can be referred to [15].

4 Simulations for Test Systems

4.1Introduction of Test Systems

The correctness and effectiveness of the proposed optimal model and method are demonstrated using the simulations for the following two test systems which are shown in Fig.1. In Fig.1 (a), the IEEE 30-bus system is divided into two areas, and the information of the transmission interfaces between the two areas is shown in Table 1. In Fig.1 (b), the IEEE 118×2-bus system consists of two IEEE 118-bus systems which are represented using two cycles, and each IEEE118-bus system has the same topology structure and parameters. For the IEEE118×2-bus system, the bus number of the area2 is the original number adding 118. The information on the transmission interfaces between the two areas is shown in Table 1 too.

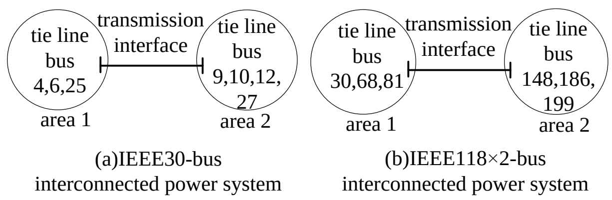

Fig. 1: Information on the two test systems

Table 1. Transmission interface information on the test system

Test system	Tie line of the transmission interface	The set value of active power of transmission interface /p.u.
IEEE30	6-9 6-10 4-12 25-27	0.5
IEEE118×2	30-148 68-186 81-199	1.0

To guarantee the set value of active power for each transmission interface, each area should have generators that can regulate the active power output. These generators are called frequency regulation units. The number of frequency regulation units is shown in Table 2. And the limit of the active power output for these generators is shown in Table 2 too.

Table 2. The number and active power outputs limit of the slack generator in each test system

Test system	The frequency regulation units in each area	The limit of the active power output of frequency regulation units /p.u.	
IEEE30	1,1	area1	area2
		(0, 3)	(0, 0.5)
IEEE118×2	1,1	area1	area2
		(0, 8)	(0, 8)

4.2 Analysis of Simulations

Firstly, the power flow operation result is obtained by using the Newton-Raphson method. And the initial active power of each transmission interface can be achieved, which is shown in Table 3.

Table 3. Initial active power of each interface

Test system	Initial value of active power of each transmission interface/p.u.
IEEE30	0.5272
IEEE118×2	0.0177

From Table 3, it can be found that the initial active power has a large difference from the set value for the two test systems. It will need a lot of work if the traditional power flow calculation is used to regulate the active power of each transmission interface. What's more, this method can't guarantee the optimal operation of the system and the operational feasibility of each variable.

According to the proposed method in Section 2 and Section 3, the model of optimal power flow considering the active power constraints of transmission interfaces is established, and the decomposition-coordination interior point method is adopted to solve the model. Meanwhile, the centralized algorithm, which is the prediction-correction primal dual interior point method, is used to solve the model too. The tolerance error for the complementary gap is 10^{-6} for the two methods.

For the two methods, solving the correction equation with reduced order is a critical aspect affecting the computation time of the algorithm. The higher dimension of the coefficient matrix in the correction equation, the more time it takes to solve the modified equation. The dimension of the coefficient matrix in the correction equation with reduced order for the two methods is shown in Table 4. When the scale of the system is increasing, the dimension of the coefficient matrix in the correction equation increases sharply for the centralized method. This increases the time of solving the correction equation and the data storage of the computer. In the decomposition-coordination interior point method, because the system is divided, the dimension of the coefficient matrix in the correction equation of each area is greatly reduced compared with the centralized algorithm, which greatly reduces the time of solving the correction equation in each area and reduces the data storage of the computer.

Table 4. Coefficient matrix dimensions of the corrected equations of the two algorithms

Test system	Centralized method	Decomposition-coordination interior point method
	Dimension of the coefficient matrix in reduced order modified equation	Dimension of the coefficient matrix in reduced order modified equation in each area
IEEE30	134	81, 90

IEEE118×2	1224	657, 645

The optimization results of the decomposition-coordination interior point method and centralized method are shown in Table 5, in which the active power loss of test systems calculated through the decomposition-coordination interior point method is consistent with the result obtained by the centralized method.

In Table 5, the number of iterations of the decomposition-coordination interior point method is more than that of the centralized method. This is due to the need for continuous interaction and coordination of the boundary variables of each area.

Table 5. Simulation results of the two algorithms

Test system	Centralized method			Decomposition-coordination interior point method				
	Number of iteration	Active power loss/p.u.	Computing time/s	Number of iteration	Active power loss /p.u.	Computing time /s	The active power output of frequency regulation unit/p.u.	
IEEE 30	9	0.1225	7.559	16	0.1225	7.661	area1	area2
							2.1324	0.4242
IEEE 118×2	12	2.1316	12.802	18	2.1316	13.073	area1	area2
							3.861	5.8906

In Table 5, the computing time of the decomposition-coordination interior point method is slightly more than that of the centralized computing method, because the simulation analysis in this paper is completed in serial computing mode. If it can be carried out in the parallel mode, the decomposition-coordination interior point method should have less computing time than the centralized computing method. The reason is as follows: on the one hand, in the calculation process of the decomposition-coordination interior point method, the order of the coefficient matrix in the correction equation for each area is greatly reduced and the amount of calculation is reduced too, which can also be seen from Table 4; On the other hand, the optimization calculation for each area can be carried out simultaneously in parallel computing mode, which can further reduce the computing time of the decomposition-coordination interior point method.

The active power output of frequency regulation units is also shown in Table 5. Compared to Table 2, it can be found that the final active power output of these generators is within their operation constraints while ensuring that the active power flowing in each transmission interface is consistent with the transaction power constraint.

Therefore, it can be seen from Table 5 that satisfactory results can be obtained using the proposed model and method with a few iterations. And it does not take a lot of time to repeatedly adjust the control variables in the system. Furthermore, the optimization results are consistent with that of the centralized algorithm, which shows that the proposed optimal power flow model and algorithm are correct and effective.

5 Conclusion

This paper presents an optimal power flow model and algorithm considering active power constraints of transmission interfaces. The proposed model considers equality constraints of power flow, active power constraints of transmission interfaces, and operational constraints of each variable. Compared with the traditional power flow calculation method, it can save time to adjust the system to satisfy various operation constraints, and it can guarantee optimal operation of the power system. Considering the multi-area characteristic of interconnected power systems, a decomposition-coordination model is established and calculated through the decomposition-coordination interior point method, which further improves the computational efficiency of the proposed optimal model. Furthermore, the method can also achieve calculation accuracy equivalent to the centralized method. Therefore, the proposed model, as well as the algorithm has a certain reference value for the operation schedule decision of the interconnected power system.

The following research work for this paper includes two aspects:
1) The data of the actual interconnected power system should be used for modeling and simulation to prove the practicability of the proposed model as well as its algorithm.
2) The feasibility of the proposed model as well as the algorithm should be verified for interconnected power systems containing renewable energy.

References:

[1] K. Xie, Y. H. Song, E. Yu, Decomposition model and interior point method for optimal spot pricing of electricity in deregulation environments, *IEEE Transactions on Power Systems*, Vol.15, No.1, 2000, pp. 39-50.

[2] M. Schmitz, P. Bernardon, J. Garcia, et al, Price-based dynamic optimal power flow with an emergency repair, *IEEE Transactions on Smart Grid*, Vol.14, No.12, 2020, pp. 1-14.

[3] M. Garcia, H. Nagarajan, R. Baldick, Generalized convex hull pricing for the AC optimal power flow problem, *IEEE Transactions on Control of Network Systems*, Vol.7, No.3, 2020, pp.1500-1510.

[4] P. N. Biskas, A. G. Bakirtzis, Decentralized congestion management of interconnected power systems, *IEE Proceedings on Generation, Transmission and Distribution*, Vol.149, No.4, 2002, pp. 432-438.

[5] Y. L. Xu, H. B. Sun, H. D. Liu, et al, Distributed solution to DC optimal power flow with congestion management, *International Journal of Electrical Power & Energy Systems*, Vol.95, 2018, pp. 73-82.

[6] S. Kim, R. Salkuti, Optimal power flow based congestion management using enhanced genetic algorithms, *International Journal of Electrical and Computer Engineering*, Vol.9, No.2, 2019, pp. 875-883.

[7] M. Dashtdar, M. Najafi, M. Esmaeilbeig, Calculating the locational marginal price and solving optimal power flow problem based on congestion management using GA-GSF algorithm, *Electrical Engineering*, Vol.3, 2020, pp. 1-18.

[8] N.Sukalkar, S.Warkad, Available transfer capability based transmission pricing using optimal power flow approach in the deregulated electricity market, *International Journal of Innovative Research in Electrical, Electronics, Instrumentation and Control Engineering*, Vol.5, No.7, 2017, pp. 41-45.

[9] J.Liu, Y.Liu, G.Qiu, et al. Learning-aided optimal power flow based fast total transfer capability calculation, *Energies*, Vol.15, No.4, 2022, pp. 1-14.

[10] A. Santisj, G. R. M. Costa, Optimal power flow solution by Newton's method applied to an augmented Lagrangian function, *IEE Generation, Transmission and Distribution*, Vol.142, No.1, 1995, pp. 33-36.

[11] X. H. Yan, V. H. Quintana, Improving an interior-point-based OPF by dynamic adjustments of step sizes and tolerances, *IEEE Transactions on Power Systems*, Vol.14, No.2, 1999, pp. 709-717.

[12] R. Baldick, B.H. Kim, A comparison of distributed optimal power flow algorithms, *IEEE Transactions on Power Systems*, Vol.15, No.2, 2000, pp. 599-604.

[13] D. Hur, Evaluation of convergence rate in the auxiliary problem principle for distributed optimal power flow, *IEE Proceedings - Generation Transmission and Distribution*, Vol.149, No.5, 2002, pp. 525-532.

[14] D. Hui, T. Lin, Q.Y. Li, et al, Decentralized optimal power flow based on auxiliary problem principle with an adaptive core, *Energy Reports*, Vol.8, 2022, pp. 755-765.

[15] W. Yan, L. L. Wen, W. Y. Li, et al, Decomposition-coordination interior point method and its application to multi-area optimal reactive power flow, *International Journal of Electrical Power & Energy Systems*, Vol.33, No.1, 2011, pp. 55-60.

Contribution of Individual Authors to the Creation of a Scientific Article (Ghostwriting Policy)
The author contributed in the present research at all stages from the formulation of the problem to the final findings and solution.

Sources of Funding for Research Presented in a Scientific Article or Scientific Article Itself
No funding was received for conducting this study.

Conflicts of Interest
The author has no conflicts of interest to declare that is relevant to the content of this article.